

# IMPROVING SATELLITE QUICKBIRD-BASED IDENTIFICATION OF LANDSCAPE ARCHAEOLOGICAL FEATURES THROUGH TASSELED CAP TRANSFORMATION AND PCA.

R. Lasaponara<sup>a\*</sup>, N. Masini<sup>b</sup>

<sup>a</sup> IMAA CNR, c.da S. Loja 85050 Tito Scalo – Potenza Italy (lasaponara@imaa.cnr.it)

<sup>b</sup> IBAM CNR, c.da S. Loja 85050 Tito Scalo – Potenza Italy (n.masini@ibam.cnr.it)

**KEY WORDS:** Remote Sensing, Archaeology, QuickBird, Satellite, High resolution, Multispectral, Identification, Processing.

## ABSTRACT:

In this paper, the Tasseled Cap Transformation (TCT) was applied to QuickBird multispectral images for extracting archaeological features linked to ancient human transformations of the landscape. The investigation was performed on Metaponto, one of the most important archaeological sites in the South of Italy. The analysis was focused on the identification of ancient land divisions likely related to Greek colonization. The obtained results showed that the use of TCT and PCA successfully enhanced the spectral information content of satellite QuickBird data; thus, allowing the detection of archaeological features with a high level of detail

## 1. INTRODUCTION

The reconstruction of ancient landscape represents an important issue not only in the field of archaeology, but, also for botany, forestry, soil science and hydrology. Information on the impacts of human actions upon the environment can be widely used to address issues in human settlement, to better understand environmental interaction, climate change, the Earth's system.

The importance of applying space technology to cultural heritage and archaeological research has been paid great attention worldwide, mainly because very high resolution (VHR) satellite data such as, IKONOS (1999) and QuickBird (2001), are able to match with aerial photogrammetric images. Actually, QuickBird is the commercial satellite that provides images with the highest spatial resolution from both panchromatic (61-72cm) and multispectral (2.44-2.88m) sensors.

One of the main advantages of satellite QuickBird data compared to aerial photos, is the possibility of exploiting the multispectral properties of the data. The spectral capability coupled with high spatial resolution can make the VHR satellite images a valuable data source for archaeological investigation ranging from small details (i.e. single subsurface building) to a synoptic view (i.e. from landscape archaeology). Recent studies performed by Lasaponara and Masini (2005, 2006) analyzed the capability of QuickBird imagery in reconstructing the urban shape of buried settlements up to single building scale. The current paper deals with the use of QuickBird images for investigations addressed to the detection of features linked to ancient human changes of the landscape. The satellite data were processed using the Tasseled Cap Transformation (TCT) and the Principal Component Analysis (PCA) for a study case located in the Metaponto territory in the Southern Italy.

## 2. ANALYSIS RATIONALE AND TOOLS

The satellite-based identification of spatial features linked to the presence of buried archaeological remains is one of the most

complex and challenging tasks faced by computer vision and photogrammetry communities. This is due to the fact that archaeological deposits tend to induce small spatial and spectral anomalies, that can be characterized by various kinds of marks, such as, soil, crop and shadow marks (Dassie, 1978; Wilson, 1982; Bewley, 2003). These marks are generally not evident on the ground, but, they could be only recognized from air. The visibility of such marks strongly depend on vegetation cover, soil types, illumination conditions and view geometry.

In this study, the Tasseled Cap Transformation (TCT) and the Principal Component Analysis were adopted for extracting archaeological features linked to ancient human transformations of the landscape.

### 2.1 Tasseled Cap Transformation

The TCT, also known as Kauth-Thomas technique, was devised for enhancing spectral information content of satellite data. The reader is referred to Crist and Kauth (1986), for an introduction. The TCT is a linear affine transformation substantially based on the conversion of given input channel data set in a new data set of composite values. The transformation depends on the considered sensor. The original TCT was derived (Kauth and Thomas, 1976) for the four bands of the Landsat MSS sensor. Later, the TCT was extended to the Landsat TM (Crist and Cicone, 1984), ETM (as available, for example, in a routine of geomatica, PCI software) and IKONOS sensor (Horne 2003). All the existing TCTs are performed on a pixel basis to best show the underlying structure of the image by using weighted sums of the input channels. Among the available weighted sums, the processing of Quickbird spectral channels was performed in two different ways. Firstly, we adopted the weighted sums devised for ETM imagery (solely considering the values for the BLUE, GREEN, RED, NIR channels), see equations 1 to 3; and, secondly, those specifically developed for IKONOS data (see equations 4 to 7). Note, that usually there are just three composite variables tasseled cap transform bands that are often used:

---

\* Corresponding author. This is useful to know for communication with the appropriate person in cases with more than one author.

- TCT-band 1
- TCT-band 2
- TCT-band 3

In particular, TCT-band 1 is a weighted sum of all spectral bands and can be interpreted as the overall brightness or albedo at the surface. TCT-band 2 primarily measures the contrast between the visible bands and near-infrared bands and is similar to a vegetation index. The TCT-band 3 can be interpreted as a measure of soil and plant moisture.

The weighted sums, adapted from the ETM input channels, are listed in equations 2 to 4 :

$$\text{TCT}_{\text{ETM}}\text{-band 1} = 0.1544 \text{ BLUE} + 0.2552 \text{ GREEN} + 0.3592 \text{ RED} + 0.5494 \text{ NIR} \quad (1)$$

$$\text{TCT}_{\text{ETM}}\text{-band 2} = -0.1009 \text{ BLUE} - 0.1255 \text{ GREEN} - 0.2866 \text{ RED} + 0.8226 \text{ NIR} \quad (2)$$

$$\text{TCT}_{\text{ETM}}\text{-band 3} = 0.3191 \text{ BLUE} + 0.5061 \text{ GREEN} + 0.5534 \text{ RED} + 0.0301 \text{ NIR} \quad (3)$$

The weighted sums developed by Horne (2003) for IKONOS input channels:

$$\text{TCT}_{\text{IKONOS}}\text{-band 1} = 0.326 \text{ BLUE} + 0.509 \text{ GREEN} + 0.560 \text{ RED} + 0.567 \text{ NIR} \quad (4)$$

$$\text{TCT}_{\text{IKONOS}}\text{-band 2} = -0.311 \text{ BLUE} - 0.356 \text{ GREEN} - 0.325 \text{ RED} + 0.819 \text{ NIR} \quad (5)$$

$$\text{TCT}_{\text{IKONOS}}\text{-band 3} = -0.612 \text{ BLUE} - 0.312 \text{ GREEN} + 0.722 \text{ RED} - 0.081 \text{ NIR} \quad (6)$$

$$\text{TCT}_{\text{IKONOS}}\text{-band 4} = -0.650 \text{ BLUE} + 0.719 \text{ GREEN} - 0.243 \text{ RED} - 0.031 \text{ NIR} \quad (7)$$

## 2.2 Principal Component Analysis

The PCA is a linear transformation which decorrelates multivariate data by translating and/ or rotating the axes of the original feature space, so that the data can be represented without correlation in a new component space (Richards, 1989). In order to do this, the process firstly computes the covariance matrix (S) among all input time series channels, then eigenvalues and eigenvectors of S are calculated in order to obtain the new feature components.

$$\text{cov}k_1, k_2 = \frac{1}{nm \sum_{i=1}^n \sum_{j=1}^m (SB_{I,J,K1} - \mu_{K2})(SB_{i,j,k2} - \mu_{k2})} \quad (8)$$

where k1, k2 are two input spectral channels, SB i,j, spectral value of the given channel in row i and column j, n number of row, m number of columns,  $\mu$  mean of all pixel SB values in the subscripted input channels.

The percent of total dataset variance explained by each component is obtained by formula 9.

$$\% i = 100 * \frac{\lambda_i}{\sum_{i=1} \lambda_i} \quad (9)$$

where  $\lambda_i$  are eigenvalues of S

Finally, a series of new image layers (called eigenchannels or components) are computed (formula 10) by multiplying, for each pixel, the eigenvector of S for the original value of a given pixel in the input bands.

$$P_i = \sum_{k=1} P_k u_{k,i} \quad (10)$$

where  $P_i$  indicates a spectral channel in component i,  $u_{k,i}$  eigenvector element for component i in input band k,  $P_k$  spectral value for channel k, number of input band.

A loading, or correlation R, of each component i with each input date k can be calculated by using formula 11.

$$R_{k,i} = u_{k,i} (\lambda_i)^{\frac{1}{2}} (\text{var}_k)^{\frac{1}{2}} \quad (11)$$

where  $\text{var}_k$  is the variance of input date k (obtained by reading the kth diagonal of the covariance matrix)

The PCA transforms the input multispectral bands in new component that should be able to make the identification of distinct features and surface types easier. The major portion of the variance in a multi-spectral data set is associated with homogeneous areas, whereas localised surface anomalies will be enhanced in later components, which contain less of the total dataset variance. This is the reason why they may represent information variance for a small area or essentially noise and, in this case, it must be disregarded. Some problems can arise from the fact that eigenvectors can not have general and universal meaning since they are extracted from the series.

## 3. SATELLITE DATA PROCESSING

### 3.1 Study area

The investigation was performed in San Salvatore which is a site 8 km from the Ionian coast, near the greek town of Metaponto in the Basilicata Region (see figure 1).

In this territory several archaeological campaigns performed in the last forty years stated human presence since the half of the 8th century B.C. when Metaponto was founded by Greeks coming from Acaia region (see Adamesteanu, 1974). Between the Greek colonization (700 BC-200 BC) and the Roman age (200 BC – 400 AD) the territory was characterized by an intense human presence, as revealed by the several rural sites brought to light by excavations, and also by the presence of an extensive system of parallel land divisions (Adamesteanu, 1973). In particular, these lines are thought to have been a network of country lanes or drainage canals (Carter, 1983; Carter, 1990). The satellite-based detection of these land divisions is the main objective of the current study.

The site investigated (see figure 1) is near to a burial site dating back between the 5th century and the middle of the 3th century. It is characterized by scarce vegetation when the satellite images were acquired.

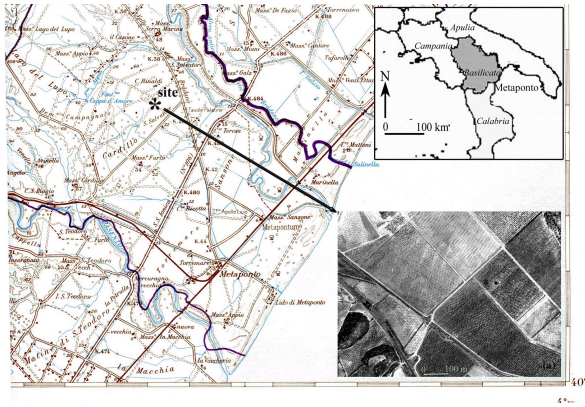


Figure 1. Location of the study area. On the bottom-right the QuickBird panchromatic image at 2.44 m spatial resolution.

### 3.2 Results

The identification of superficial anomalies was performed by a visual inspection. On the basis of the single spectral QuickBird bands, the signs of ancient land divisions are more evident from the red channel (see figures 2a,b) and the panchromatic (see figures 3a,b).

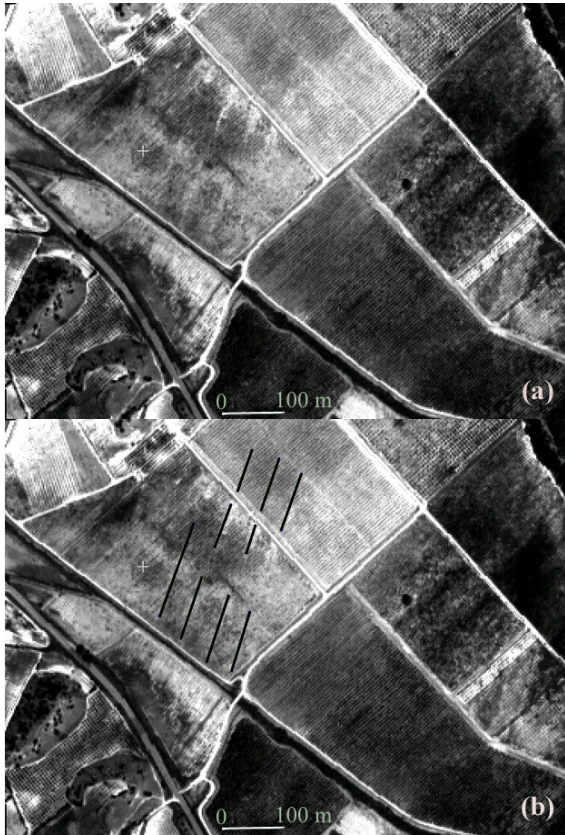


Figure 2. San Salvatore in Metaponto: (a) QuickBird red channel image at 2,44 m spatial resolution and (b) detected land divisions.

This was not surprising, since the panchromatic has a higher spatial resolution (at 0.61 m in the current acquisition), whereas the QuickBird red channel was experienced (Lasaponara and Masini, 2005) to be highly capable to emphasize archaeological features over bare soil. Actually, the area under investigation did not have significant vegetation cover when the satellite imagery were acquired.

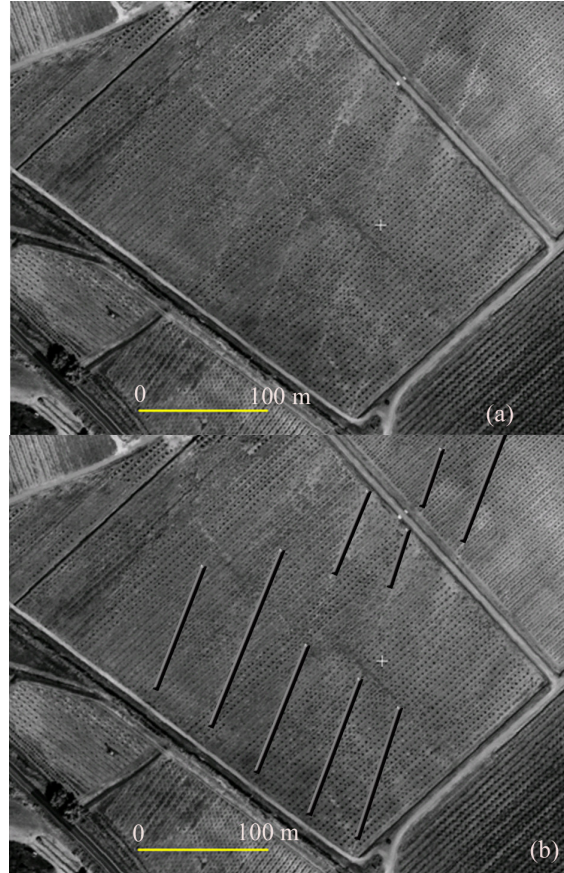


Figure 3. San Salvatore in Metaponto: (a) panchromatic image (at 0,61 m spatial resolution) and (b) detected land divisions.

It is expected that the TCT bands should provide improved enhancement of archaeological marks. In the current case under investigation, the best image enhancements were obtained from TCT<sub>ETM</sub>-band 1 (see figures 4a,b) and TCT<sub>ikonos</sub>-band 1 (see figures 5a,b), followed by TCT<sub>ETM</sub>-band 3 (see figures 6a,b). Whereas, unsatisfactory results were obtained from TCT<sub>ETM</sub>-band 2, and TCT<sub>ikonos</sub>-band 2,3,4.

The first TCT bands tend to capture meaningful variations well describing the data. The first TCT bands (both TCT<sub>ETM</sub>-band1 and TCT<sub>ikonos</sub>-band1, see figures 4 and 5) give feature enhancements very close each other. Both of them are very similar to the QuickBird panchromatic image even with a lower spatial resolution (at 2,44 m). The first component obtained from both the TCTs (see, equation 1, and 4) is a weighted sum of all bands in the direction of principal variation in soil reflectance, thus including more soil reflectance or brightness information. For this reason, it is really surprising the fact that the first TCT bands contain little more information not evident at higher resolution in the pan image.

The second TCT bands, both  $TCT_{ETM}$ -band 2 and  $TCT_{ikonos}$ -band 2, were not able to extract meaningful features of any interest. This was widely expected being that these TCT bands are the greenness axis, which tend to describe the spectral contrast (mainly emphasized in the NIR band) between the bare soil and areas covered by vegetation. Such a contrast was not present in the image for the area under investigation that was scarcely vegetated when the satellite images were acquired.

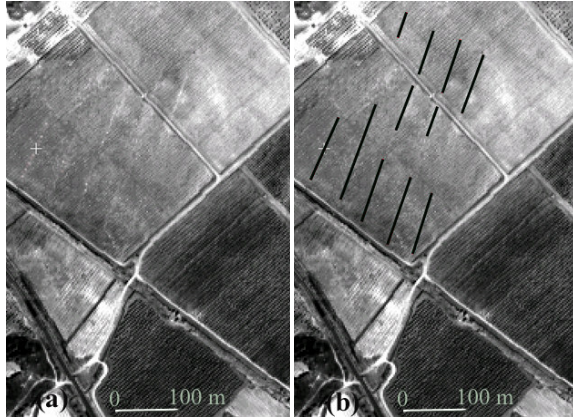


Figure 4. San Salvatore in Metaponto: (a)  $TCT_{ETM}$  band1 and (b) detected land divisions.

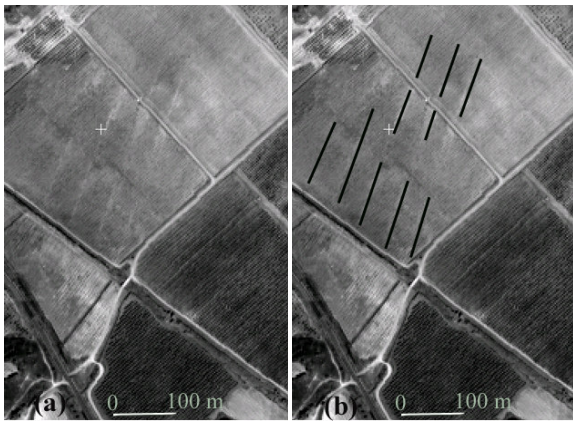


Figure 5. San Salvatore in Metaponto: (a)  $TCT_{ikonos}$  band 1 and (b) detected land divisions.

The  $TCT_{ETM}$ -band 3 (see figure 6 a,b) was capable to enhance the linear features of drainage canals that are generally characterized by higher brightness values due to the presence of subsurface material. Such a material, composed by rubblestones, tends to reduce soil humidity content; thus, increasing the spectral values compared to the surrounding areas. This behaviour substantially confirms the early experimental findings (Crist and Cicone, 1984) which pointed out that an increasing in soil moisture content tends to induce a decreasing in both brightness and wetness values. Conversely, drier soils tend to increase values in both of the two TCT components (brightness and wetness).

Finally, the  $TCT_{ikonos}$ -band 3,4 did not emphasize any features of archaeological interest. This can be explained as follows. Compared to the third  $TCT_{ETM}$ -band (see equation 3),  $TCT_{ikonos}$ -band 3 (see equation 6) is obtained using different weighted coefficients and arithmetic combinations. In other

words, in  $TCT_{ETM}$ -band 3 all the different spectral contributes are summed, whereas in  $TCT_{ikonos}$ -band 3, the BLUE, GREEN and NIR weighted contributes were subtracted to red channel one. Such a spectral combination (equation 6) did not appear to be capable of distinguishing variability in the soil moisture content. Finally, the fourth  $TCT_{ikonos}$ -band 4 did not provide any interesting results.

The application of PCA to the four QuickBird spectral images provides a new set of four uncorrelated components. Unfortunately, the interpretation of such components does not have a general and universal meaning since they are extracted from the series itself. PCA provided the best results in its component 1. A visual comparison among the TCT bands and PCA component 1 (Figure 7) clearly shows the fact that PCA provides a better separability of the archeological features compared to those extracted from the TCT products. Nevertheless, at the same time, compared to the TCT products, PCA made a smaller number of archaeological marks visible (see, for example, figure 6 related  $TCT_{ETM}$  band3).

PCA component 2 was less significant and it allowed to extract a less number of features compared to PCA 1.

Finally, the later component were characterized by very low variance. They were essentially noise without any interesting information of archeological interest, and were disregarded.

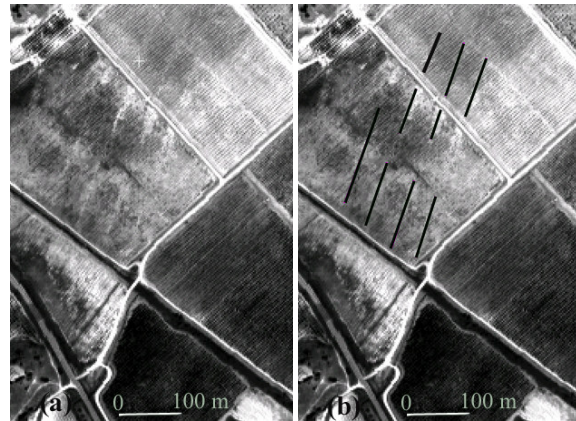


Figure 6. San Salvatore in Metaponto: (a)  $TCT_{ETM}$  band3 and (b) detected land divisions.

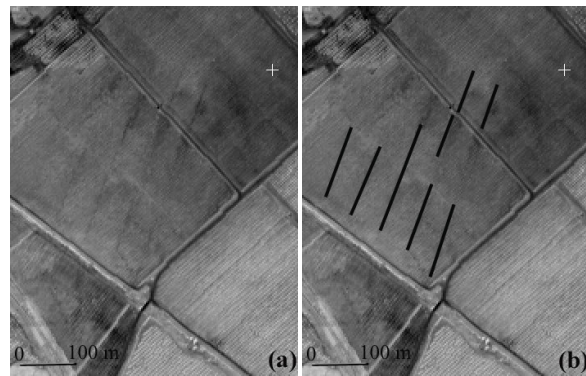


Figure 7. San Salvatore in Metaponto: (a) PCA1 and (b) detected land divisions.

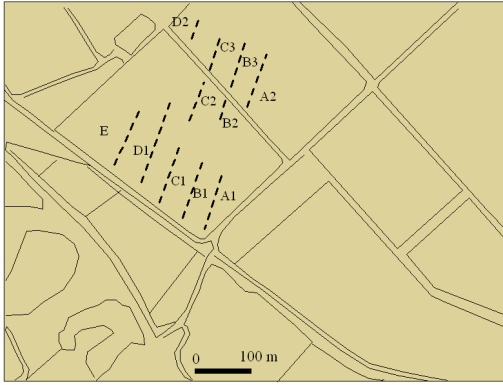


Figure 8. San Salvatore in Metaponto: dashed lines indicate the land divisions detected by using the data listed in the table 1.

As a whole, Figure 8 and Table 1 resume the land divisions identified by using panchromatic, red channel, TCT<sub>ETM</sub> band1, TCT<sub>ETM</sub> band3, TCT<sub>IKONOS</sub> band1 and PCA1. The results showed that the use of TCT and PCA successfully allow a qualitative and quantitative improvement in the identification of archaeological marks

#### 4. FINAL REMARKS

Ancient land divisions represent one of the most significant traces of the human transformation of landscape which need to be protected. Unfortunately, due to destructive effects of mechanized agriculture, these archaeological signs are increasingly difficult to identify by using solely panchromatic aerial images. In this paper, we investigated the feasibility of using TCT and PCA for processing satellite QuickBird multispectral images to enhance these archaeological features linked to ancient human activity. The investigation was performed on Metaponto, one of the most important archaeological sites in the South of Italy. Our results pointed out that the use of TCT and PCA successfully allow an improved identification of land divisions.

| Feature | length (m) | Features detected for each data |     |                       |                       |                          |       |
|---------|------------|---------------------------------|-----|-----------------------|-----------------------|--------------------------|-------|
|         |            | Pan (0,6)                       | Red | TCT <sub>etm</sub> b1 | TCT <sub>etm</sub> b3 | TCT <sub>ikonos</sub> b1 | PCA 1 |
| A1      | 100,6      | X                               | X   | X                     | X                     | X                        | X     |
| A2      | 98,32      | X                               | X   | X                     | X                     | X                        | X     |
| B1      | 112,7      | X                               | X   | X                     | X                     | X                        | X     |
| B2      | 48,19      | X                               | X   | X                     | X                     | X                        | X     |
| B3      | 88,93      | X                               | X   | X                     | X                     | X                        | X     |
| C1      | 104        | X                               | X   | X                     | X                     | X                        | X     |
| C2      | 74,65      | X                               | X   | X                     | X                     | X                        | X     |
| C3      | 70,84      |                                 | X   | X                     |                       | X                        |       |
| D1      | 159,8      | X                               | X   | X                     | X                     | X                        | X     |
| D2      | 41,74      |                                 |     | X                     |                       |                          |       |
| E       | 107,5      | X                               |     | X                     |                       | X                        | X     |

Table 1. Land divisions detected by using panchromatic, red channel, TCT<sub>ETM</sub> band1, TCT<sub>ETM</sub> band3 and TCT<sub>IKONOS</sub> band1.

#### REFERENCE

- Adamesteanu, D., 1973. Le suddivisioni di terra nel metapontino in *Problèmes de la terre en Grèce ancienne*, Mouton, Paris, pp. 49-61.
- Adamesteanu, D., 1974. *La Basilicata antica. Storia e monumenti*, Cava dei Tirreni.
- Bewley, R.H., 2003. Aerial survey for archaeology. *Photogrammetric Record*, 18 (104), pp. 273-292.
- Carter, J. C., 1983. *The territory of Metaponto 1981-82*, Institute of Classical Studies, Austin.
- Carter, J. C., 1990. Between the Bradano and Basento: Archaeology of an Ancient Landscape. In *Earth Patterns. Essays in Landscape Archaeology*, W. Kelso and R. Most (Ed.), University of Virginia Press, Charlottesville, pp. 227-243.
- Crist, E.P. and Cicone, R.C., 1984. A Physically-Based Transformation of Thematic Mapper Data – The TM Tasseled Cap. *IEEE Transactions of Geoscience and Remote Sensing*, 22(3), pp. 256-263.
- Crist, E.P. and Kauth, R.J., 1986. The Tasseled Cap De-Mystified. *Photogrammetric Engineering and Remote Sensing*, 52 (1), pp. 81-86.
- Dassie, J., 1978. *Manuel d'archeologie aerienne*, Editions Technip, Paris.
- Horne, J., 2003. A Tasseled Cap Transformation for IKONOS Images. In: *Proceedings of the ASPRS: 2003 Annual Conference and Technology Exhibition*.
- Kauth, R.J. and Thomas, G.S. 1976. The Tasseled Cap – a graphical description of the spectral-temporal development of agricultural crops as seen by Landsat. In *Proceedings of the Symposium on Machine Processing of Remotely Sensed Data*, Purdue University, West Lafayette, Indiana, pp. 4B41-4B51.
- Lasaponara, R. and Masini, N., 2005. QuickBird-based analysis for the spatial characterization of archaeological sites: case study of the Monte Serico Medioeval village. *Geophysical Research Letter*, 32(12), L12313 10.1029/2005GL022445.
- Lasaponara, R. and Masini, N., 2006. On the potential of Quickbird data for archaeological prospection. *International Journal of Remote Sensing*, 27, 3607-3614.
- Richards, J. A. 1986. *Remote Sensing Digital Image Analysis.*, Springer-Verlag.
- Wilson, D.R., 1982. *Air photo interpretation for archaeologists*, St. Martin's Press, London.